Wireless Pers Commun (2017) 95:4243–4256
DOI 10.1007/s11277-017-4077-7

Main Effects Ensured by Symmetric Circular Slots Etched on the Radiating Patch of a Compact Monopole Antenna on the Impedance Bandwidth and Radiation Patterns

Mohamed Hayouni[1] · Fethi Choubani[1] · Tan-Hoa Vuong[2] · Jacques David[2]

Published online: 10 March 2017

Abstract Three compact monopole ultrawideband (UWB) antennas with half-wavelength symmetric circular slots etched on the radiating patch and operating in the UWB spectrum are proposed. Parametric studies followed by experimental results of the return loss coefficient S_{11} versus the circular slot length prove dual ensured functions. In fact, a switching from an impedance mismatch to an impedance matching appears when we replace a semicircular etched slot by a small circular slot while maintaining its inner radius constant. Simulated and measured reflection coefficient S_{11} of a fabricated prototype with a stack of two small circular slots concord well and prove an impedance bandwidth enhancement that covers 3.9–14 GHz frequencies band ($S_{11} < -10$ dB) compared to the impedance bandwidth 3.55–4.77 and 7.65–11.08 GHz ($S_{11} < -10$ dB) of the baseline antenna without slots. In addition, measured radiation patterns in the H-plane of the monopole with two etched symmetric slots, are stably omnidirectional at 5.8 and 7.5 GHz. It is noted that due to some strong transverse currents around the small circular symmetric embedded slots, the cross-polarization in the same plane and at the same frequencies are not as low as single monopole. We noticed that there appears to be a close correspondence between the minimum of E_Φ and the maximum of E_θ electrical components. That is to say, the signals of the co-polarizations are irrelevant to those of the cross-polarizations. Due to

✉ Mohamed Hayouni
mohamed.hayouni@supcom.rnu.tn

Fethi Choubani
fethi.choubani@supcom.rnu.tn

Tan-Hoa Vuong
Tan-Hoa.Vuong@enseeiht.fr

Jacques David
Jacques.David@enseeiht.fr

[1] Innov'Com Research Laboratory, Higher School of Communications (Sup'Com), City of Communications Technology, University of Carthage, Raoued Road, Km 3.5, 2083 Ariana, Tunisia

[2] LAPLACE – Plasma and Energy Conversation Laboratory, UMR5213, INPT-ENSEEIHT, 2 Street Charles Camichel, Postbox 7122, 31071 Toulouse, Cedex 7, France

its impedance matching and its stable omnidirectional radiation patterns, reliability and the reduced occupation volume, the proposed printed monopole with two etched small symmetric circular slots is suitable for the emerging applications of the wireless technology.

Keywords Cross-polarization · Impedance matching · Symmetric circular slot · Transverse currents · Radiation patterns · Ultrawideband (UWB)

1 Introduction

Since the Federal Communications Commission (FCC) first approved rules and allocated 3.1–10.6 GHz spectrum for the commercial use of ultrawideband (UWB) in 2002, implementation and design of UWB systems and especially UWB antennas, considered as an essential part of these UWB systems, has become highly competitive. Several UWB antenna designs adopting various techniques are recently deployed in the literature [1–7] and are widely used for omnidirectional radiation in UWB wireless communications. However, wireless communication systems require particular electromagnetic wave polarization. So, design multiband and broadband circular polarizer is considered an important method that can transfer the linear to-circular polarized wave under a normal incidence of plane wave [8–11]. Nevertheless, there is a risk of possible electromagnetic interferences (EMI), as over the allocated spectrum to be spanned by antennas. This EMI problem occurred due to existing narrowband communication systems, such as the world interoperability for microwave access WiMAX operating in 3.3–3.7 GHz, the wireless local area network WLAN operating in 5.15–5.285 GHz, and downlink of X-band satellite communication systems operating in 7.25–7.75 GHz. A simpler method used to solve this problem is to design UWB antenna with band-notched characteristics. Several UWB antennas with band-stop function have been reported in the literature, mostly with one band-stop function for WLAN [12, 13]. It has been demonstrated that by incorporating U-shaped [14–18], arc-shaped [15, 19], C-shaped [20] or stepped slots in the radiating patch or in the ground plane a band-stop function is achieved mostly for WLAN. One notched band is also achieved by using a pair of compact split ring resonators (SRRs) loaded on the back side of a CPW fed printed circular monopole [21]. Modal analysis of band-stop UWB antennas, proposed in [18], demonstrates the existence of resonant modes dependent on the incorporated narrowband slot structure (slot modes), whose location within the planar radiating patch estimates the effect over the behavior of the monopole. Both switchable and tunable band-notched UWB antennas have been then proposed by electronically controlling the excitation of the first mode. Recently, several antennas with dual notched bands or triple notched bands were reported in the literature. It has been demonstrated that WiMAX and WLAN dual notched bands are achieved with two short-circuited folded stepped impedance resonators (SIRs) printed on the front surface of a partial grounded substrate on both sides of the feed line of a circular patch antenna [22].WiMAX and WLAN dual notched bands are also achieved using a UWB slot antenna and L- and J-shaped parasitic elements [23] or by etching two C-shaped slots on the radiation patch with limited area [24]. Moreover, by integrating a pair of I-shaped and L-shaped stubs in the square slots of the ground plane of a rectangular patch antenna and placing resonant open circuited stubs adjacent to the antenna border, triple band-notched are achieved at 3.6, 5.7 and 7.2 GHz with an impedance bandwidth from 2.8 to 11.7 GHz

with VSWR < 2 [25]. One, dual or triple notched bands can be also achieved by using one, two or three optimized capacitively loaded loop (CLL) resonators on both sides of the feed line [26]. Additionally, a triple band-notched UWB antenna is achieved by etching out two elliptic single complementary split-ring resonators (ESCSRRs) of different dimensions from the radiating patch of the antenna and by placing two rectangular split-ring resonators near the feed line-patch junction [27]. A set of a straight open ended quarter-wavelength slot and three semicircular half wavelength slots are etched in the radiating patch monopole to generate triple notched bands [28].

Hence, to keep the radiator footprint unaltered and compact in order to be mounted in miniature wireless communications systems such as wireless cameras used by people contributing geo-tagged [29], usually designers choose the approach of etching different shaped slots in the radiating patch or in the ground plane. Indeed, in [30] semicircular slots etched in the radiating patch of a UWB antenna are used to notch two narrow bands. However, keeping the same inner radius, circular physical length adjustment effects on impedance matching, current distributions and radiation patterns of these etched circular slots haven't been yet investigated.

In this paper, using our previously baseline reported antenna [30], we re-examine firstly circular convex corners effects on antenna's input impedance in its real and imaginary two parts. Afterwards, we will review the impact of the half-wavelength semicircular slot reported in [31], as an impedance mismatching tool, etched in the radiating patch of the baseline antenna, on the input impedance of the monopole. Next, circular slot physical length reduction effect on the impedance bandwidth of the antenna will be analyzed to reveal its second role as an impedance matching tool. Measured radiation patterns of a monopole's prototype with two optimized small circular slots will be then investigated, proving the importance of the strong transverse current distributions around the small symmetric circular slots. Finally, the evaluation of the group delay, which is another critical parameter for UWB antenna that measures the time signal distortion brought by the antenna, will be evaluated.

1.1 Design Evolution

Using our baseline antenna (without slots) reported in [30], three slotted antennas are designed in three stages as depicted by Fig. 1. All designed antennas have overall dimensions of $35 \times 30 \times 1.52$ mm^3. Each radiating patch is printed on a partial grounded FR4 substrate of a relative permittivity $\varepsilon_r = 4.32$, 30×35 mm^2 dimensions, loss tangent $\tan \delta = 0.02$ and 1.52 mm thickness. Each antenna is fed through a microstrip feed line along the (xz) major axis without gap to the ground plane and whose length is the same as the width of the partial ground plane (11.5 mm). The initial design (configuration A) reported in [31] has a semicircular slot S_1 of 1 mm width, $R_1 = 5$ mm inner radius and $L_{S1} = \pi.\ (R_1 + 1/2)$ physical length but the second one (Configuration B) shows the etched slot S_1 with an optimized reduced physical. The final design (Configuration C) contains a second circular S_2 above the first optimized etched slot S_1 of L_{S2} physical length. Namely, in all designs, the slots positions are kept symmetric along the width of the antenna and have a common center that coincides with that of the monopole to ensure circularity of the radiation patterns. Along with the three designs, on the right of Fig. 1, corresponding realizations are also presented.

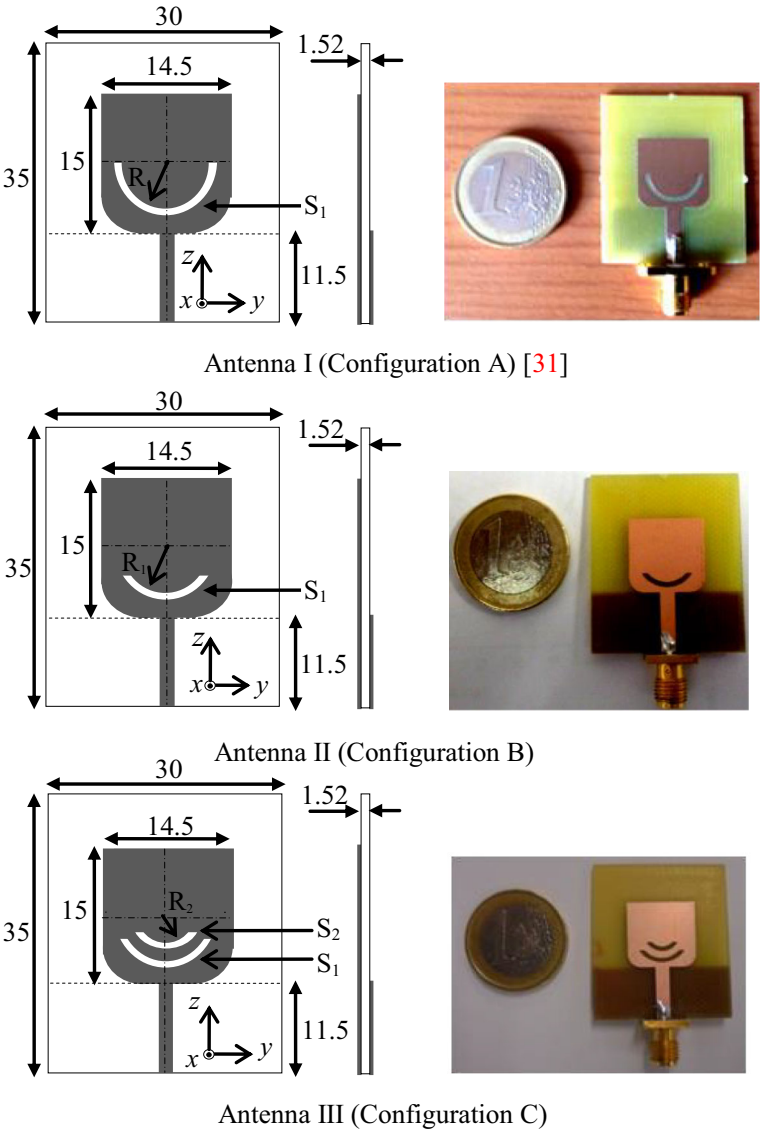

Fig. 1 Slotted antenna evolution and photographs of corresponding prototypes

2 Results and Discussions

2.1 Baseline Antenna (Without Slots)

Starting from our recently published monopole printed antenna reported in [30] (antenna without slots), we present in this paper the simulated real and imaginary parts of the input impedance Z_{in} in order to assess the convex circular corners effects on the impedance matching of the antenna especially in the X-band. Figure 2 shows that the imaginary part

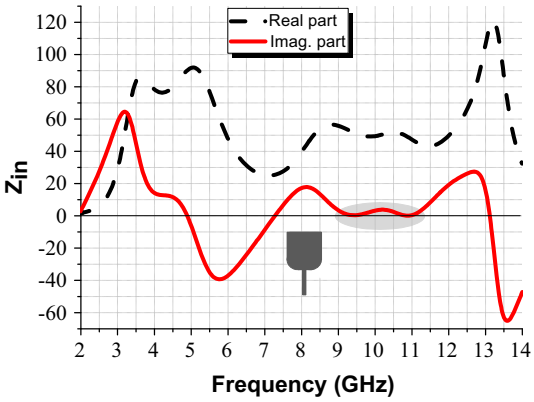

Fig. 2 Simulated input impedance Z_{in} of the baseline antenna reported in [30]

of Z_{in} touches the zero axis two times without cutting it at 9.4 and 10.6 GHz frequencies. The real part of Z_{in} remains stable between two frequencies and stays around 50 Ω. Namely the resonance of the antenna coincides with 7.3 GHz while the others zeros of the Z_{in} imaginary part over 2–14 GHz frequency range are antiresonances.

2.2 Configuration A

Figure 3 shows the reflection coefficient S_{11} of the fabricated antenna I depicted by Fig. 1. The agreement between measured and simulated performances is quite good. The measured S_{11} is less than −10 dB over 3.55–4.77 GHz (29.3%) and 7.65–11.08 GHz (36.6%) but it remains greater than −10 dB over the frequency range 4.77–7.65 GHz. A band-notched UWB antenna is then achieved. The notched band covers two narrow bands communications systems which are WLAN and downlink of X-band satellite communication systems. The semicircular slot physical length is $L_{S1} = 17.3$ mm, it is about half of the guided wavelength ($\lambda_g/2$) calculated at 5.5 GHz, namely $\lambda_g = \lambda_0/\sqrt{\varepsilon_{eff}}$ where λ_0 is the free space wavelength and $\varepsilon_{eff} = (\varepsilon_r + 1)/2$. Figure 4 shows the simulated input impedance of the configuration A design in its both real and imaginary parts. An impedance mismatching is noted at 5.5 GHz.

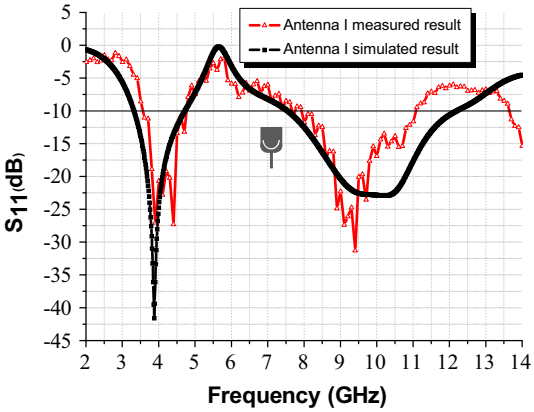

Fig. 3 Measured and simulated S_{11} results of the antenna I

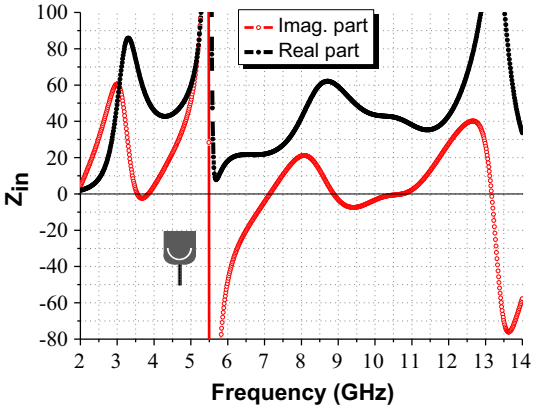

Fig. 4 Simulated input impedance Z_{in} of the antenna I

2.3 Configurations B and C

Saving the same inner radius $R_1 = 5$ mm, the impedance matching versus the circular slot physical length L_{S1} is examined. Figure 5 shows the behavior of the S_{11} versus L_{S1}. In fact, By decreasing L_{S1} from 17.3 to 10.2 mm, the central frequency of the notched band increases to higher frequencies while the corresponding S_{11} decreases to -5 dB. However, from $L_{S1} = 7.1$ mm, the circular slot improves the impedance bandwidth of the baseline antenna (without slot) reported in [30] since the S_{11} remains below -10 dB from 3.5 to 12.5 GHz. An UWB antenna is then resulted. Figure 6 shows simulated and measured S_{11} results of the antenna II with an optimized circular slot of $L_{S1} = 7.1$ mm. The agreement between the two S_{11} curves is good especially in terms of -10 dB impedance bandwidth. Nevertheless, the peaks levels of the measured S_{11} remains better than those of the simulated one. In fact, the S_{11} reached -29 and -35 dB around 7.9 and 10.6 GHz respectively. In effect, from the simulated input impedance Z_{in} of the antenna II shown by Fig. 7, a new resonance frequency 8.7 GHz appears while the second and third resonance frequencies of the baseline antenna (without slots) disappear.

The antenna III (configuration C) depicted by Fig. 1, shows another symmetric circular slot S_2 etched in the radiating patch. S_2 is characterized by its inner radius

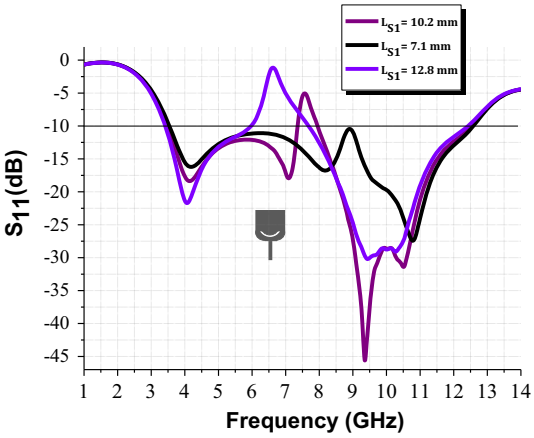

Fig. 5 L_{S1} physical length effect on S_{11} keeping the same radius $R_1 = 5$ mm

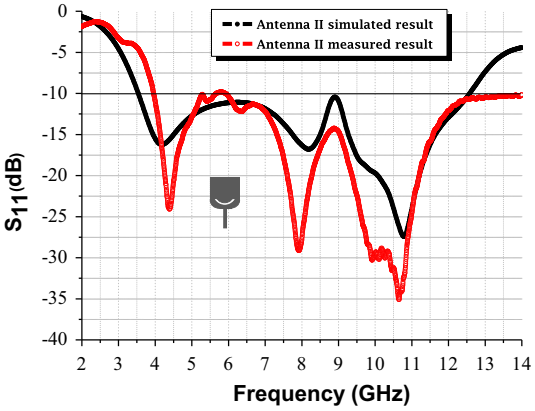

Fig. 6 Measured and simulated S_{11} results of the antenna II

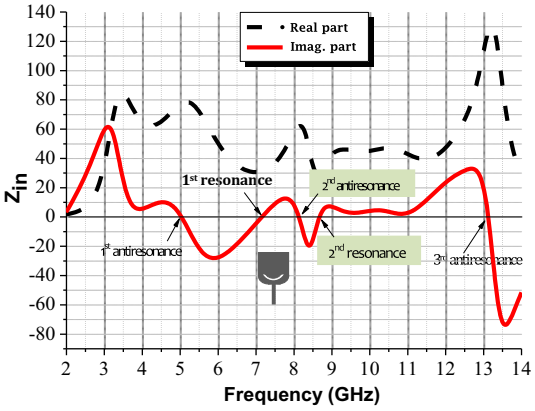

Fig. 7 Simulated input impedance Z_{in} of the antenna II

$R_2 = 3$ mm and physical length $L_{S2} = 5.9$ mm. Both measured and simulated S_{11} results, depicted by Fig. 8, concord well. Compared to the measured S_{11} of the antenna II, we note an impedance matching improvement at higher frequencies, especially over

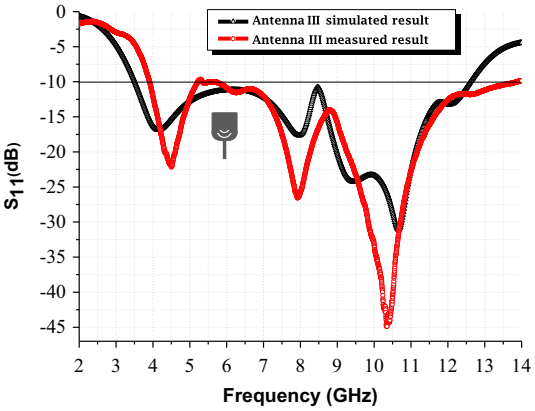

Fig. 8 Measured and simulated S_{11} results of the antenna III

the frequencies band 9.5–10.6 GHz, since the S_{11} reaches −45 dB at 10.4 GHz. Band-notching or bandwidth enhancement dual effects of symmetric circular slot, etched in the radiating patch of a printed monopole antenna, can be then achieved by selecting the adequate length of the symmetric circular embedded slots as depicted by Fig. 9. Simulated VSWR results prove that the antenna III can satisfy the requirements of VSWR < 2 over 3.47–12.8 GHz frequencies band which covers the most of the UWB spectrum allocated by the FCC while the antenna I covers nearly the same ultrawideband except for the WLAN rejected band.

To obtain the radiation characteristics, the fabricated antenna II and Antenna III have been characterized in an anechoic chamber using antenna measurement system as shown by Fig. 10. With reference to the position of the antenna in the coordinate system (Fig. 1), the radiating patch is towards the azimuth angle $\Phi = 90°$. The testing is done for all values of the elevation and azimuth angles theta and phi. The reference antenna used is a calibrated double ridged horn antenna. A MATLAB generated polar plots of the measured normalized radiation patterns in the H-plane (X–Y plane) at 5.8 and 7.5 GHz frequencies for the antennas II and III are respectively shown by Figs. 11 and 12. Radiation patterns at these two given frequencies are steadily omnidirectional. The vertical polarization is the dominant one for both antennas. However, for the antenna II, the cross-polarization levels are lower than 10 and 11 dB at 5.8 and 7.5 GHz respectively, whereas the cross-

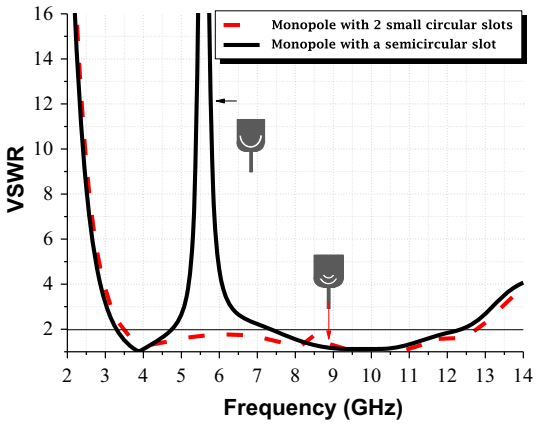

Fig. 9 Simulated VSWR of antennas I and III

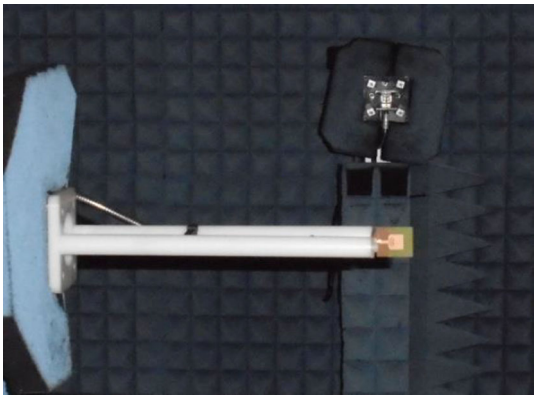

Fig. 10 Photograph of the realized antenna III in an anechoic chamber

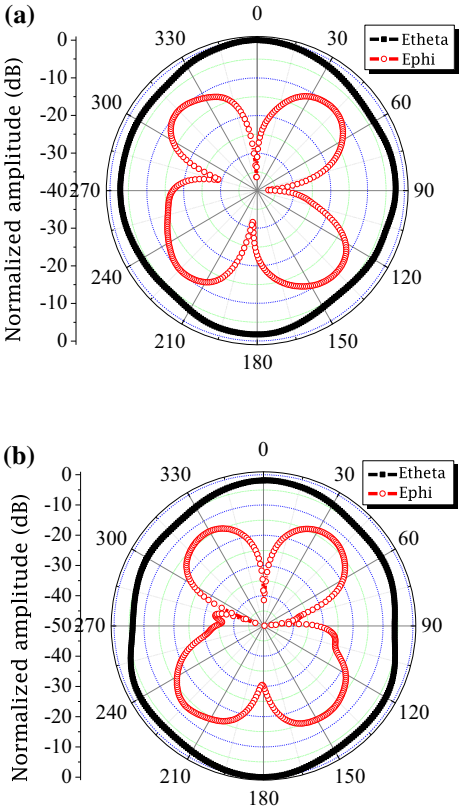

Fig. 11 Measured radiation patterns in the X–Y plane at **a** 5.8 GHz and **b** 7.5 GHz frequencies of the antenna II

polarization levels for the antenna III, are lower than 10 and 12 dB at 5.8 and 7.5 GHz respectively. It may be noted that the cross-polarization in the X–Y plane at 5.8 and 7.5 GHz is not as low as for single monopole, because there are some strong transverse currents around the circular symmetric embedded slots, as it can be seen in Fig. 13. From the H-plane radiation patterns, we notice that there appears to be a close correspondence between the minimum of E_Φ and the maximum of E_θ. That is to say, the signals of the co-polarizations are irrelevant to those of the cross-polarizations.

Another critical parameter for UWB antenna, which measures the time signal distortion brought by the antenna is the group delay. It should be constant throughout the operating band to ensure minimum distortion in the transmitted signal. Namely the group delay, as defined in [32], is the negative derivative of the transmission phase $\varphi(\omega)$ w. r. t. the angular frequency ω.

$$\tau = -\frac{d\varphi(\omega)}{d\omega} \tag{1}$$

Simulated group delay calculated between two identical prototypes over the frequency range of 2–14 GHz shows, as depicted by Fig. 14, that it remains below 1 ns while the variations are within 0.7 ns. We can consider this antenna reliable so that a transmitted signal will not be seriously distorted by the proposed monopole.

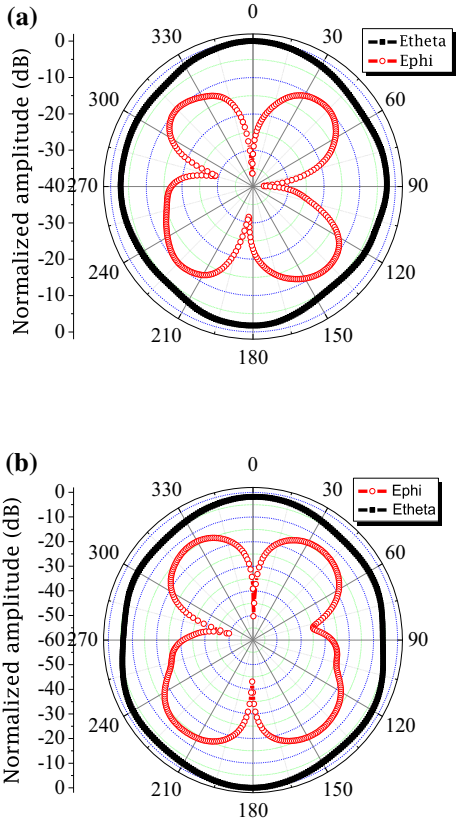

Fig. 12 Measured radiation patterns in the X–Y plane at **a** 5.8 GHz and **b** 7.5 GHz frequencies of the antenna III

3 Conclusion

In this paper, compact printed planar monopole UWB antennas were presented and investigated. Each one exhibits a simple structure. By optimizing the physical lengths of half-guided wavelength embedded circular slots, two fold objectives can be achieved. Indeed, semicircular slot incorporated in the middle of the radiating patch generates a band-notched frequency whose central frequency is determined from $\lambda_g/2$ physical length of the slot. A WLAN band-notched UWB prototype is then successively fabricated and measured. We note that the measured S_{11} at the central frequency of the rejected band 5.5 GHz reaches −2 dB. By reducing the physical length of the circular etched slot to an optimized value (7.1 mm), a simulated bandwidth of 112.5% (3.5–12.5 GHz) is achieved proving that, in addition of notching some narrow bands, circular incorporated slots can be considered as an impedance bandwidth enhancement tool. A good measured S_{11} is also achieved at the uplink of X-Band satellite communication systems (−45 dB at 10.4 GHz) by etching another symmetric slot of 5.1 mm length. Additionally, current distributions proved that embedded circular slots ensure simultaneously a reduction and an increase of vertical and horizontal currents respectively, resulting in steadily omnidirectional patterns in the H-plane at both 5.8 and 7.5 GHz frequencies. Due to its good characteristics in terms of bandwidth, impedance matching, radiation patterns, reliability so that a transmitted signal will not be seriously distorted, and miniature dimensions, the proposed printed

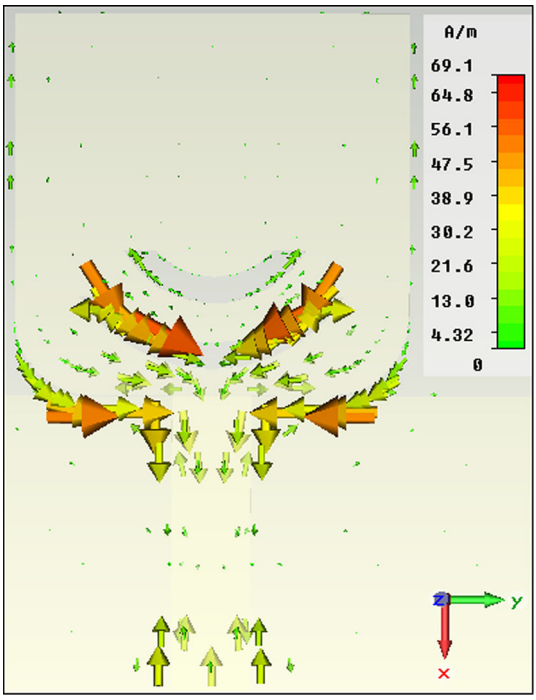

Fig. 13 Simulated current distribution of antenna III at 7.5 GHz

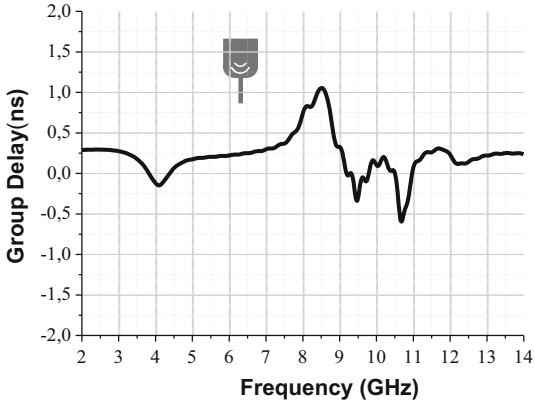

Fig. 14 Simulated group delay of the antenna with two symmetric circular slots

monopole antenna incorporating two symmetric circular slots can be useful for portable communication devices requiring vertical polarization over the entire UWB spectrum.

Acknowledgements The authors thank a lot Professor M. Ferrando-Bataller, Research members and the Technical Staff with the Instituto de Telecomunicaciones y Aplicaciones Multimedia (iTEAM) of the Universitat Politècnica de València, Spain.

References

1. Wang, L., Xu, L., Chen, X., Yang, R., Han, L., & Zhang, W. (2014). A compact ultrawideband diversity antenna with high isolation. *IEEE Antennas and Wireless Propagation Letters, 13,* 35–38.
2. Rostomyan, N., Ott, A. T., Blech, M. D., Brem, R., Eisner, C. J., & Eibert, T. F. (2015). A balanced impulse radiating omnidirectional ultrawideband stacked biconical antenna. *IEEE Transactions on Antennas and Propagation, 63*(1), 59–68.
3. Liu, J., Esselle, K. P., Hay, S. G., & Zhong, S. (2014). Effects of printed UWB antenna miniaturization on pulse fidelity and pattern stability. *IEEE Transactions on Antennas and Propagation, 62*(8), 3903–3910.
4. Kumar, R., Khokle, R. K., & Ram Krishna, R. V. S. (2014). Ahorizontally polarized rectangular stepped slot antenna for ultra wide bandwidth with boresight radiation patterns. *IEEE Transactions on Antennas and Propagation, 62*(7), 3501–3510.
5. Wang, Y. W., Wang, G. M., Yu, Z. W., Liang, J. G., & Gao, X. J. (2014). Ultra-wideband E-plane monopulse antenna using vivaldi antenna. *IEEE Transactions on Antennas and Propagation, 62*(10), 4961–4969.
6. Abadi, S. M. A. M. H., Ghaemi, K., & Behdad, N. (2015). Ultra-wideband, true-time-delay reflectarray antennas using ground-plane-backed, miniaturized-element frequency selective surfaces. *IEEE Transactions on Antennas and Propagation, 63*(2), 534–542.
7. Jamro, D. A., Hong, J., Bah, M. H., Mangi, F. A., & Memon, I. (2015). Triangular antenna with novel techniques for RCS reduction applications. *Wireless Communications, Networking and Applications, 348,* 775–782.
8. Mangi, F. A., Xiao, S., Memon, I., & Jamro, D. A. (2015). Novel design and performance analysis of broadband dual layer circular polarizer based on frequency selective surface for 60 GHZ application. *Wireless Communications, Networking and Applications, 348,* 319–325.
9. Mangi, F. A., Xiao, S., Mallah, G. A., Kakepoto, G. F., & Imran, M. (2016). Fission transmission linear-to-circular polarization conversion based on compact bi-layer structure. *Indonesian Journal of Electrical Engineering and Computer Science, 3*(3), 519–526.
10. Mangi, F. A., Xiao, S., Mallah, G. A., Jamro, D. A., Memon, I., & Kakepoto, G. F. (2016). Multiband circular polarizer based on fission transmission of linearly polarized wave for X-band applications. *Journal of Electrical and Computer Engineering*. doi:10.1155/2016/4293089.
11. Mangi, F. A., Xiao, S., Jamro, D. A., Khan, S. A., Imran, M., & Kakepoto, G. F. (2016). Manipulating electromagnetic wave linear-to-circular polarization conversion transmitter based on periodic strips array. In *3rd international information science and control engineering (ICISCE), Beijing, China.*
12. Cho, Y. J., Kim, K. H., Choi, D. H., Lee, S. S., & Park, S. O. (2006). A miniature UWB planar monopole antenna with 5-GHz band-rejection filter and the time-domain characteristics. *IEEE Transactions on Antennas and Propagation, 54*(5), 1453–1460.
13. Hong, C. Y., Ling, C. W., Tarn, I. Y., & Chung, S. J. (2007). Design of a planar ultrawideband antenna with a new band-notch structure. *IEEE Transactions on Antennas and Propagation, 55*(12), 3391–3397.
14. Cho, Y. J., Kim, K. H., Choi, D. H., Lee, S. S., & Park, S. O. (2006). A miniature UWB planar monopole antenna with 5-GHz band-rejection filter and the time-domain characteristics. *IEEE Transactions on Antennas and Propagation, 54*(5), 1453–1460.
15. Yin, K., & Xu, J. P. (2008). Compact ultra-wideband antenna with dual band stop characteristic. *Electronics Letters, 44,* 453–454.
16. Lee, W. S., Kim, D. Z., Kim, K. J., & Yu, J. W. (2006). Wideband planar monopole antennas with dual band-notched characteristics. *IEEE Transactions on Microwave Theory and Techniques, 54*(6), 2800–2806.
17. Deng, J. Y., Yin, Y. Z., Zhou, S. G., & Liu, Q. Z. (2008). Compact ultrawideband antenna with tri-band notched characteristic. *Electronics Letters, 44,* 1231–1233.
18. Antonino-Daviu, E., Cabedo-Fabrés, M., Ferrando-Batallerand, M., & Rodrigo Peñarrocha, V. M. (2010). Modal analysis and design of band-notched UWB planar monopole. *IEEE Transactions on Antennas and Propagation Antennas, 58*(5), 1457–1467.
19. Qu, X., Zhong, S. S., & Wang, W. (2006). Study of the band-notch function for a UWB circular disc monopole antenna. *Microwave and Optical Technology Letters, 48*(8), 1667–1670.
20. Chu, Q. X., & Yang, Y. Y. (2008). 3.5/5.5 GHz dual band-notch ultrawideband antenna. *Electronics Letters, 44*(3), 172–174.
21. Siddiqui, J. Y., Saha, C., & Antar, Y. M. M. (2014). Compact SRR loaded UWB circular monopole antenna with frequency notch characteristics. *IEEE Transactions on Antennas and Propagation Antennas, 62*(8), 4015–4020.

22. Sung, Y. (2012). UWB monopole antenna with two notched bands based on the folded stepped impedance resonator. *IEEE Antennas and Wireless Propagation Letters, 11,* 500–502.
23. Kueathaweekun, W., Anantrasirichai, N., Benjangkaprasert, C., Nakasuwan, J., & Wakabayashi, T. (2012). Controllable band-notched slot antenna for UWB communication systems. *ETRI Journal, 34*(5), 674–683.
24. Xu, J., Shen, D.-Y., Wang, G.-T., Zhang, X.-H., Zhang, X.-P., & Wu, K. (2012). A small UWB antenna with dual band-notched characteristics. *International Journal of Antennas and Propagation*. doi:10.1155/2012/656858.
25. Luo, K., Ding, W. P., & Cao, W. Q. (2014). Compact monopole antenna with triple band-notched characteristics for UWB applications. *Microwave and Optical Technology Letters, 56*(4), 822–827.
26. Lin, C.-C., Jin, P., & Ziolkowski, R. W. (2012). Single, dual and tri-bandnotched ultrawideband (UWB) antennas using capacitively loaded loop (CLL) resonators. *IEEE Transactions on Antennas and Propagation, 60*(1), 102–109.
27. Sarkar, S., Srivastava, K. V., & Saurav, K. (2014). A compact microstrip-fed triple band-notched UWB monopole antenna. *IEEE Antennas and Wireless Propagation Letters, 13,* 396–399.
28. Nguyen, T. D., Lee, D. H., & Park, H. C. (2011). Design and analysis of compact printed triple band-notched UWB antenna. *IEEE Antennas and Wireless Propagation Letters, 10,* 403–406.
29. Memon, I., Chen, L., Majid, A., Lv, M., Hussain, I., & Chen, G. (2015). Travel recommendation using geo-tagged photos in social media for tourist. *Wireless Personal Communications, 80*(4), 1347–1362.
30. Hayouni, M., El Oualkadi, A., Choubani, F., Vuong, T. H., & David, J. (2012). Antenna ultra wideband enhancement by non-uniform matching. *Progress In Electromagnetics Research Letters, 31,* 121–129.
31. Hayouni, M., El Oualkadi, A., Choubani, F., Vuong, T. H., & David, J. (2014). Design and analysis of a compact WLAN band-notched monopole UWB. In ACES 2014. In: *Proceeding of the 30th international review of progress in applied computational electromagnetics conference, Jacksonville, Florida, USA*.
32. Kumar, R., Khokle, R. K., & Ram Krishna, R. V. S. (2014). A horizontally polarized rectangular stepped slot antenna for ultra wide bandwidth with boresight radiation patterns. *IEEE Transactions on Antennas and Propagation, 62,* 3501–3510.

Mohamed Hayouni was born in Kef, Tunisia in 1979. He received the electrical engineering degree from École Nationale Supérieur d'Ingénieur de Tunis (ENSIT) de Tunis, Tunisia in 2002 and the M. Eng. and Ph.D. degrees in Information Technology and Communication from École Supérieure des communications de Tunis (Sup'Com), Tunisia in 2005 and 2012 respectively. Since 2005, he has been a research member with innovation of communicant and cooperative mobiles (Innov'Com) Research Laboratory, Sup'Com. In 2011, he joined Institut Supérieur d'Informatique du Kef, Université de Jendouba, Tunisia as a teaching assistant with telecommunications and he has been an assistant professor with the same institute in 2015. His main research interests include microwave, millimeter wave detection, design and optimisation techniques for ultrawideband and multiband compact antennas and numerical methods for solving electromagnetic problems.

Fethi Choubani was born in Mahdia, Tunisia in 1961. He received the electrical engineering diploma from Ecole Nationale d'Ingénieurs de Tunis, Tunisia in 1987 and the M. Eng and Ph.D. degrees from ENSEEIHT, Institut National Polytechnique de Toulouse, Toulouse, France in 1988 and 1993 respectively. Since 1993, he has been with Sup'Com, Ecole supérieure des Communications de Tunis as an assistant, associate and then professor where he taught radiofrequency components and devices, propagation and antennas, and ElectroMagnetic compatibility. His main interests are focused on oscillators and their applications to electromagnetic sensors, EMC, nonlinear devices, modelling of passive, active components and RF techniques and measurements. He has been offered a position of visiting research professor in the Department of Electrical and Computer Engineering at the University of Illinois at Urbana-Champaign in 1999 during 3 months, and in Laplace Laboratory in ENSEEIHT for one month. He was head of the Telecommunications Department, ESPTT (Tunisia) from 1995 to 1996, director of strategic studies, Tunisia Telecom (Tunisian operator in telecommunications during 1999–2001, director of High Institute of Technological studies from during 2010–2011 and advisor of ICT Minister during 2012–2014. He has published more than 100 journal and international conference papers.

Tan-Hoa Vuong obtained the rank doctor of electronics of the National Polytechnic Institute of Toulouse (INPT) in 2000, with the very honourable mention. Thesis rewarded by the price Léopold ESCANDE (INPT) and the price for thesis for the doctoral school for Toulouse. Then, he decreed the title of enabling with written research by the chancellor of the universities in 2014. Currently, he is responsible for the electronic department of IPST-CNAM-Occitanie-Midi-Pyrenees center; and professor of engineering in electronics and automatically with the IPST, where he teaches analogical and numerical electronics, the microprocessor, the DSP, telecommunication with very high flow, and the electromagnetic one… since 1998. He also teaches "the techniques of the communication of proximity" to the students of the level masters, and the formation training: electronics, embarked system, telecommunication. He works at the Laboratory of Laplace—UMR 5213 (ENSEEIHT-UPS) of the ENSEEIHT since 1997 on the measurement techniques out of HF and microwaves of low and strong power, on the mobile communication system, like on the microwaves sensors. He is interested in electromagnetic applied to the medical and military environment.

Jacques David was born in France in 1946. He received the Ph.D. degree in electronics from the University of Toulouse, Toulouse, France, in 1974 and the Docteur es Sciences Degree from the National Polytechnic Institute of Toulouse, in 1984. He is currently a professor Emeritus of Electrical Engineering at the National Polytechnic Institute of Toulouse (ENSEEIHT). Since 1971, he has been working at the Electronics Laboratory of ENSEEIHT and his primary interest is in the field of electromagnetic wave propagation with applications in the electromagnetic compatibility domain and wave-matter interaction.